Probing Dense, Compact Dark Globules[1]

Amelia M. Stutz[2], George H. Rieke[2], John H. Bieging[2], Jocelyn Keene[3], Mark Rubin[4], Yancy L. Shirley[2], Thangasamy Velusamy[4], Michael W. Werner[4] and David J. Wilner[5]

ABSTRACT

We present *Spitzer* observations of two globules: CB190 (L771) and B335 (CB199). In the case of **CB190** we observe a roughly circular 24μm shadow with a 70$''$ radius. The extinction profile of this shadow matches the profile derived from 2MASS photometry at the outer edges of the globule and reaches a maximum of $\sim$32 visual magnitudes at the center. The corresponding mass of CB190 is $\sim$10 $M_\odot$. Our HHT ^{12}CO and ^{13}CO J = 2-1 data over a 10$'\times$10$'$ region centered on the shadow show a temperature $\sim$ 10 K. Bonnor-Ebert fits to the density profile, in conjunction with this distance, yield $\xi_{max} = 7.2$, indicating that CB190 may be unstable. The high temperature (56 K) of the best fit Bonnor-Ebert model is in contradiction with the CO and thermal continuum data, leading to the conclusion that the thermal pressure is not enough to prevent free-fall collapse. We also find that the turbulence in the cloud is inadequate to support it. However, the cloud may be supported by the magnetic field, if this field is at the average level for dark globules. Since the magnetic field will eventually leak out through ambipolar diffusion, it is likely that CB190 is collapsing or in a late pre-collapse stage. A detailed discussion of our analysis can be found in Stutz et al. (2007). In the case of **B335** we observe an 8μm shadow which we interpret as evidence for a flattened molecular core with a diameter $\sim$8000 AU, a structure predicted by models and distinct from the previously detected protoplanetary disk, with radius $\sim$200 AU (Stutz et al., 2008, in preparation).

---

[1]This work is based in part on observations made with the *Spitzer Space Telescope*, which is operated by the Jet Propulsion Laboratory, California Institute of Technology, under NASA contract 1407.

[2]Department of Astronomy and Steward Observatory, University of Arizona, 933 North Cherry Avenue, Tucson, Arizona 85721; astutz@as.arizona.edu.

[3]Caltech, Pasadena, 91125

[4]Jet Propulsion Lab, California Institute of Technology, 4800 Oak Grove Drive, Pasadena, CA 91109.

[5]Harvard-Smithsonian Center for Astrophysics, 60 Garden Street, Cambridge, MA 02138

Subject headings: ISM: globules – ISM: individual (CB190) – infrared: ISM – (ISM:) dust, extinction

1. Introduction

Compact and dense dark globules have the potential to collapse into stars. Their density profiles have been studied by measuring near infrared extinction of background starts (e.g., Harvey et al. 2001; Alves et al. 2007). However, we know of very few examples that appear to be collapsing yet do not already have young stars at their cores. Is this gap in our knowledge because of observational selection effects, or is the process very rapid, making it difficult to catch a globule doing it? Near infrared extinction maps are limited probes of very dense globules because they lose sensitivity at high extinctions and small angular scales.

These limitations can be overcome using shadows cast by globules in Spitzer observations at 8, 24 and even 70 μm. There are a number of globules with prominent shadows that appear to bridge the gap between static clouds and YSO's.

We present the case of CB190. In the outer regions, our shadow analysis is in good agreement with near-IR extinction measurements; however, the shadow remains sensitive to high-density and compact material in the core, with 30 mags of extinction in V. We measured CO emission with the Heinrich Hertz Submm Telescope (HHT). Our analysis shows that the dense core of CB 190 cannot be supported by thermal or turbulent pressure. Magnetic pressure might supply the deficit, but if so it is likely to be temporary (1 - 10 Myr) because of ambipolar diffusion. Thus, it appears that CB 190 is either collapsing or in a pre-collapse state (Stutz et al. 2007).

We also compare the properties of CB190 with similar measurements of the archetypal star-forming globule, Barnard 335.

2. CB190: an example of a 24μm shadow

Cold cloud cores, where star formation begins, represent the stage in early stellar evolution after the formation of molecular clouds and before the formation of Class 0 objects. Their emission is inaccessible at shorter wavelengths, such as the near infrared and visual bands, due to low temperatures, very high gas densities, and associated large amounts of dust. Because cold cloud cores can best be observed at sub-millimeter and far-infrared wavelengths, these spectral regions are essential to developing an understanding of the first steps toward star-formation (see, e.g., Bacmann et al. 2000; Kirk et al. 2007). The wavelength

range accessible to the *Spitzer* Space Telescope, 3.6 μm to 160 μm, is ideally suited to observe cold, dense regions.

CB190 (L771), centered at about RA = $19^h20^m48^s$, Dec = $+23^o29'45''$, is an example of one such dark globule and is classified in the Lynds catalog as having an opacity of 6 (Lynds 1962), i.e., very high. Clemens & Barvainis (1988) study this object as part of an optically selected survey of small molecular clouds. They find that it appears optically isolated, is somewhat asymmetric ($a/b \sim 2.5$) and has some bright rims of reflection and Hα. CB190 is $\sim 5'$ across, and has an estimated distance of 400 pc (Neckel et al. 1980).

CB190 was observed with the MIPS instrument (Rieke et al. 2004) at 24 μm, 70 μm and 160 μm, *Spitzer* program ID 53 (P.I. G. Rieke). The observations were carried out in scan map mode. Figure 1 shows these data, along with the Digital Sky Survey (DSS) red plate image of the globule.

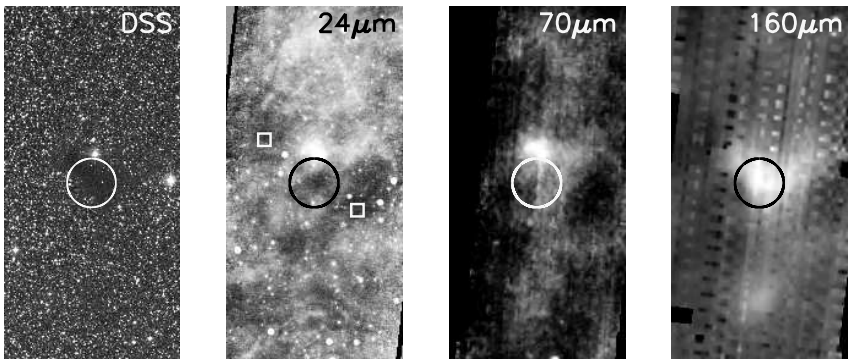

Fig. 1.— Gallery of CB190 data. The images are centered on the 24μm shadow at RA = $19^h20^m48^s$, Dec = $+23^o29'45''$, and are oriented such that north is up and east is to the left. The images have a height of $24'$ and a width of $12'$. The corresponding wavelengths are labeled in the top right corners. The optical image is from the red Digital Sky Survey. All four images are marked with a $100''$ circle centered on the location of CB190.

The CB190 region was mapped in the J=2-1 transitions of ^{12}CO and ^{13}CO with the 10-m diameter HHT on Mt. Graham, Arizona on 2005 June 9. A $10' \times 10'$ field centered at RA = $19^h20^m49.5^s$, Dec = $+23^o29'57''$ was mapped. In figure 2 we show two maps of the integrated ^{12}CO and ^{13}CO J=2-1 lines. Furthermore, in figure 3, we show the ^{13}CO J=2-1 contours overlaid on the 24 μm image; the spatial coincidence between the two is evident.

To better constrain the CO line properties, we observed the core of the molecular cloud with high velocity resolution with the HHT. The position observed was at RA = $19^h20^m46.4^s$, Dec = $+23^o29'45\farcs6$, which is the peak of the ^{12}CO intensity map (fig. 2). We also obtained C^{18}O J = 2 - 1 observations from the CSO (Michael M. Dunham, private communication,

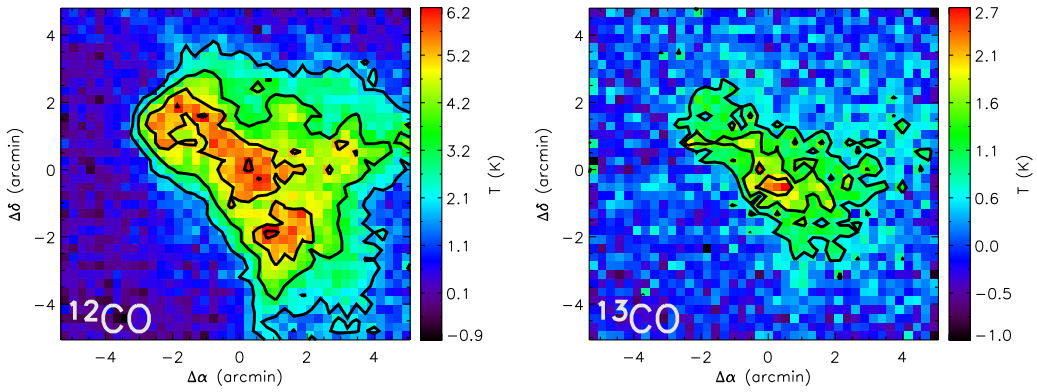

Fig. 2.— Maps of the integrated ^{12}CO (J = 2-1, $\nu = 220.399$ GHz) and ^{13}CO (J = 2-1, $\nu = 230.538$ GHz) lines taken with a FWHM telescope resolution of 32″ and convolved to a square grid cell spacing of 16″. The central coordinates of the images are RA = $19^h20^m49^s$, Dec = $+23^o29'57''$. The color-bars indicate the temperature scales in each map. The ^{12}CO contour levels are 2, 3.5, 5, and 6 K, and the ^{13}CO contour levels are 0.8, 1.4, and 2.0 K.

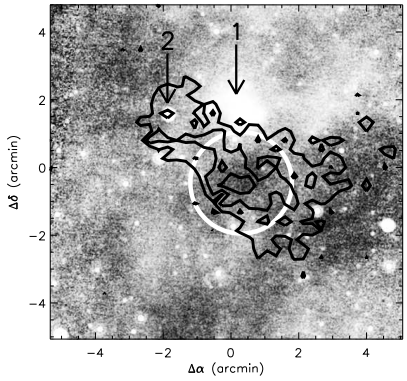

Fig. 3.— 24 μm image with ^{13}CO contours overlaid. The image is $\sim 10'$ on a side. The ^{13}CO contour levels are 0.8, 1.4, and 2.0 K. The white circle is centered on the 24μm shadow and the peak of the ^{13}CO emission.

2006).

We derive an extinction profile based on the 24 μm shadow; our profile is in good agreement with the 2MASS stellar extinction values. We show both in fig. 4. To test the stability of CB190, we perform Bonnor-Ebert profile fits to the 24 μm profile. Our best-fit model is shown in fig. 5.

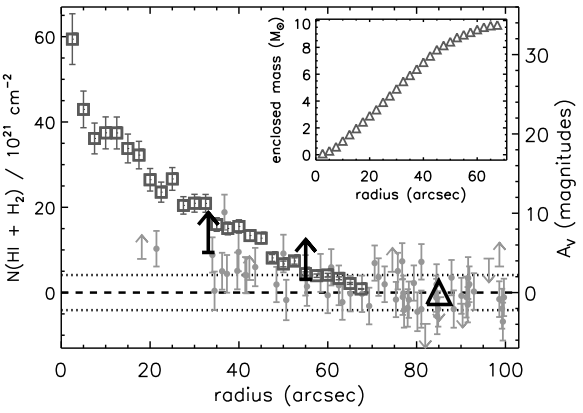

Fig. 4.— Comparison of the CB190 column density profiles: the 24 μm shadow profile is shown with dark grey squares, and the individual 2MASS stellar A_V estimates are marked with light grey filled circles. The black symbols indicate the best-fit Gaussian mean values for the 2MASS data in three radial bins, inside 40″, 40″ to 70″, and 70″ to 100″, and are plotted versus the average radius in each respective bin; the two inner-most points are shown as lower limits (black arrows) because of the inclusion of individual 2MASS lower limits in the best-fit Gaussian calculation. The inset shows the corresponding enclosed mass for the 24 μm extinction profile.

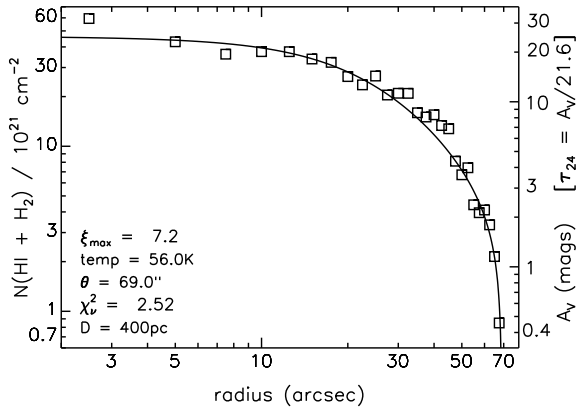

Fig. 5.— The 24 μm column density profile (squares) is shown with the best-fit Bonnor-Ebert model (solid line). The errors in the data are about the size of the squares. The best-fit model parameters are indicated: temperature T = 56.0 K, θ_{max} = 69.″0, and ξ_{max} = 7.2. The right-hand-side vertical axis indicates the magnitudes of visual extinction, or equivalently, τ_{24}, the optical depth at 24 μm. The implied mass for the globule is $\sim$10 $M_\odot$, about twice the Jeans Mass. The fitted temperature is unrealistically high given the dust temperature of $\sim$10 to 12 K and the CO temperature of 10 K.

We have combined Spitzer MIPS and IRAC data with HHT and GBT millimeter data of CB190 and arrive at the following conclusions (further details in Stutz et al., 2007):

• We introduce a method for studying the structure of cold cloud cores from the extinction shadows they cast at 24 μm.

• We derive an A_V profile of the 24 μm shadow that is in good agreement with the reddening estimates derived from the 2MASS data at the outer edges and reaches a maximum value of $\sim$32 visual magnitudes through the center.

• The mass measured from the optical depth profile is a factor of $\sim$2 greater than the Jeans mass for this object.

• We fit Bonnor-Ebert spheres to our A_V profile. The temperature required for thermal support is is far in excess of the dust and gas temperatures we measure. From our measured line widths, turbulence is probably inadequate to support the cloud. However, magnetic support may be enough to prevent collapse.

These pieces of evidence together form a consistent picture in which CB190 is a cold dark starless core. Although collapse cannot be halted with thermal and turbulent support alone, the magnetic field may contribute enough energy that it could support CB190 against collapse. Hence, magnetic field support should be included in evaluating the stability of other cold cloud cores. CB190 appears to be at an interesting evolutionary phase. It may be in the first stages of collapse (if the magnetic field is weaker than average). Alternately, if it is currently supported by magnetic pressure, it is expected that collapse may begin in some ten million years as the magnetic field leaks out of the globule by ambipolar diffusion.

3. B335: an example of a 8 μm shadow

We observe an 8 μm shadow just to the south of the prototypical Class 0 source B335 (see fig. 6). The geometry of B335 is such that this shadow lies in the region where one might expect to find a structure resembling a flattened molecular core. Such structures, distinct from the protoplanetary disk (typically a few hundred AU in extent), are predicted to be large ($\sim$ 1000 AU). Three-dimensional numerical simulations generally show that cloud collapse proceeds quickly into filaments, or disks with spiral arms, and with typical dimensions of 1000 AU (diameter) (Whitehouse & Bate 2006; Krumholz et al. 2007; Arreaga-Garcia et al. 2007), a result that was also anticipated in some earlier work (e.g., Nelson & Langer 1997). The interstellar medium around a forming star becomes organized into two distinct classes of structure: 1.) an evolving, pseudo-stable protoplanetary disk of size up to a couple of hundred AU; and 2.) what we will term a flattened molecular core to include the variety of filaments, disks, and spiral arms produced by the simulations, and of typical size 1000 AU. Viewed edge-on, most versions of flattened molecular cores would appear as linear structures

similar to edge-on disks.

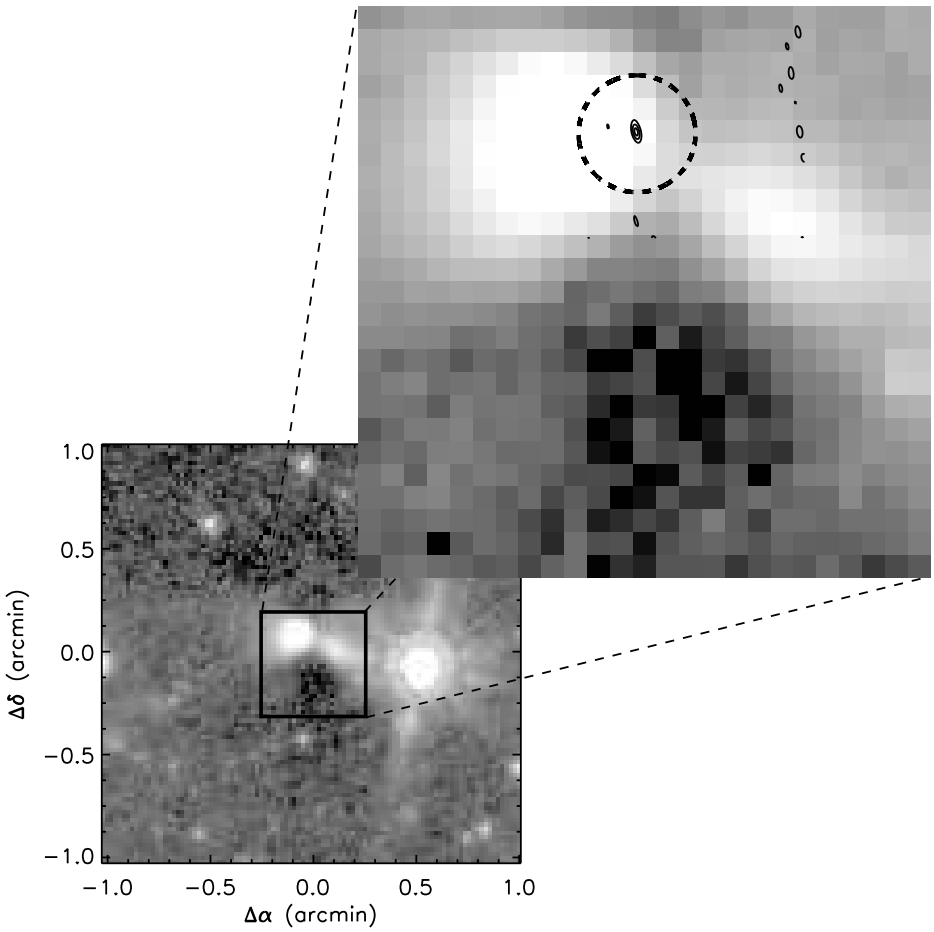

Fig. 6.— IRAC 8 μm image of B335, with inset, both shown at the original mosaic pixel scale of $1\farcs2$ pix^{-1}. An 8 μm shadow can be observed near the center and just south of the protostar. *Inset:* $30'' \times 30''$ in size; the solid contours indicate the location of the circumstellar disk ($\sim$ 200 AU), observed at 1.2 mm by Harvey et al. (2003a); the dashed circle with $3''$ radius indicates the 24 μm PSF.

In B335 we see evidence of both the flattened molecular core and the protoplanetary disk. The disk is detected in emission in the IRAM interferometer continuum image of Harvey et al. (2003a), with a diameter of about 200 AU (see fig. 6), as is typical for more evolved examples (Andrews & Williams 2007). The flattened molecular core appears as a shadow in the IRAC data with a radius of order 4000 AU ($\sim 20''$), the distance from the Harvey et al. (2003a) position of the protostar and the edge of the 8 μm shadow (see fig. 6). It is likely that this flattened molecular core is filtered out by the interferometer and that single dish images do not have enough resolution to detect it cleanly.

Portions of this work were carried out at the Jet Propulsion Laboratory, California Institute of Technology, under contract with the National Aeronautics ans Space Administration. This work was supported by contract 1255094 issued by Caltech/JPL to the University of Arizona.

REFERENCES

Alves, J., Lombardi, M., & Lada, C. J. 2007, A&A, 462, L17

Andrews, S. M., & Williams, J. P. 2007, ApJ, 659, 705

Arreaga-García, G., Klapp, J., Sigalotti, L. D. G., & Gabbasov, R. 2007, ApJ, 666, 290

Bacmann, A., André, P., Puget, J.-L., Abergel, A., Bontemps, S., & Ward-Thompson, D. 2000, A&A, 361, 555

Clemens, D. P., & Barvainis, R. 1988, ApJS, 68, 257

Harvey, D. W. A., Wilner, D. J., Lada, C. J., Myers, P. C., Alves, J. F., & Chen, H. 2001, ApJ, 563, 903

Harvey, D. W. A., Wilner, D. J., Myers, P. C., & Tafalla, M. 2003a, ApJ, 596, 383

Harvey, D. W. A., Wilner, D. J., Myers, P. C., Tafalla, M., & Mardones, D. 2003b, ApJ, 583, 809

Kirk, J. M., Ward-Thompson, D., & André, P. 2007, MNRAS, 375, 843

Krumholz, M. R., Klein, R. I., & McKee, C. F. 2007, ApJ, 665, 478

Lynds, B. T. 1962, ApJS, 7, 1

Neckel, T., Klare, G., & Sarcander, M. 1980, A&AS, 42, 251

Nelson, R. P., & Langer, W. D. 1997, ApJ, 482, 796

Rieke, G. H., et al. 2004, ApJS, 154, 25

Stutz, A. M., et al. 2007, ApJ, 665, 466

Whitehouse, S. C., & Bate, M. R. 2006, MNRAS, 367, 32